Faraday Discussions

Accepted Manuscript

This manuscript will be presented and discussed at a forthcoming Faraday Discussion meeting. All delegates can contribute to the discussion which will be included in the final volume.

Register now to attend! Full details of all upcoming meetings: http://rsc.li/fd-upcoming-meetings

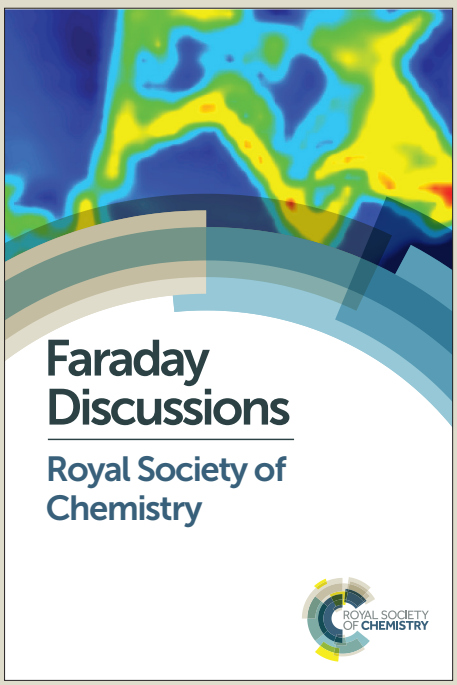

This is an *Accepted Manuscript*, which has been through the Royal Society of Chemistry peer review process and has been accepted for publication.

Accepted Manuscripts are published online shortly after acceptance, before technical editing, formatting and proof reading. Using this free service, authors can make their results available to the community, in citable form, before we publish the edited article. We will replace this *Accepted Manuscript* with the edited and formatted *Advance Article* as soon as it is available.

You can find more information about *Accepted Manuscripts* in the Information for Authors.

Please note that technical editing may introduce minor changes to the text and/or graphics, which may alter content. The journal's standard Terms & Conditions and the Ethical guidelines still apply. In no event shall the Royal Society of Chemistry be held responsible for any errors or omissions in this *Accepted Manuscript* or any consequences arising from the use of any information it contains.

ROYAL SOCIETY OF CHEMISTRY

www.rsc.org/faraday_d

Surface plasmon enhanced energy transfer between gold nanorods and fluorophores: application to endocytosis study and RNA detection

Yinan Zhang[1§¶], Guoke Wei[2§], Jun Yu[3], David J. S. Birch[1] and Yu Chen[1*]

[1]Department of Physics, Strathclyde University, John Anderson Building, 107 Rottenrow, Glasgow G4 0NG, UK

[2]Department of Physics, Beihang University, Beijing 100191, China

[3] Strathclyde Institute of Pharmacy and Biomedical Sciences, University of Strathclyde, Glasgow G4 0RE, UK

*corresponding author, email: y.chen@strath.ac.uk

§ both authors made the same level of contribution to this work.

Abstract

Previously we have demonstrated surface plasmon enhanced energy transfer between fluorophores and gold nanorods under two-photon excitation using fluorescence lifetime imaging microscopy (FLIM) in both solution and intracellular phases. These studies demonstrated that gold nanoparticle-dye energy transfer combinations are appealing, not only in Förster resonance energy transfer (FRET) imaging, but also energy transfer-based fluorescence lifetime sensing of bio-analytes. Here, we apply this approach to study the internalization of gold nanorods (GNRs) in HeLa cells using early endosome labeling marker GFP. Observed energy transfer between GFP and GNRs indicates the involvement of endocytosis in GNR uptake. Moreover, a novel nanoprobe based on oligonucleotide functionalized gold nanorod for nucleic acid sensing via dye-GNRs energy transfer is demonstrated, potentially opening up new possibilities in cancer diagnosis and prognosis. The influence of oligonucleotide design on such nanoprobe performance was studied for the first time using time-resolved fluorescence spectroscopy, bringing new insight to the optimization of the nanoprobe.

Keywords: Gold nanorods; Energy transfer; FLIM; RNA; Endocytosis.

I. INTRODUCTION

Förster resonance energy transfer (FRET) is frequently referred to as the 'spectroscopic ruler' and has been applied to a broad range of research, including distance distributions, metabolic sensing, protein and cell functions [1-2]. It occurs between donors and acceptors in close proximity, with an effective range of typically 1-8 nm for organic donors and acceptors, as limited by the nature of their dipole-dipole interaction. However, this constraint in the length scale of detection can be extended dramatically

when metallic particles act as acceptors since the distance dependence now scales at less than the 6^{th} power [3].

In addition to extending the upper range limit, gold nanoparticles are in many ways superior to organic dye molecules in energy transfer application as they are photostable. This combines with low toxicity, tunable absorption band and ability to conjugate to bio-molecules, making gold nanoparticles a versatile probe in biological imaging and sensing [4-15]. This is especially true for gold nanorods (GNRs), where their strong two-photon luminescence (TPL) makes them excellent fluorescence probes in biological imaging [16, 17] as the intrinsic advantages of two-photon excitation (high spatial definition, increased specificity, reduced photo-bleaching and reduced excitation of endogenous fluorescence) can also be brought to bear. Previously we demonstrated that by incorporating GNRs in cells their fast fluorescence decay time of GNRs could be used to good effect to increase contrast in Fluorescence Lifetime Imaging Microscopy (FLIM) [18].

Recent studies in energy transfer processes in Au nanoparticle assemblies have shown their applications in protein binding and conformational changes, RNA folding/unfolding, metal ion detection, etc [19]. While most studies used single photon excitation, we have reported the study of energy transfer between dye and GNRs under two-photon excitation. Energy transfer between 4'-6-Diamidino-2-phenylindole (DAPI), a commonly used DNA dye, and GNR were observed under two-photon excitation using FLIM in both solution and intracellular phases [15]. It was also found that GNRs provided more efficient energy transfer than gold nanospheres with comparable size and concentration. This energy transfer enhancement was attributed to the longitudinal surface plasmon mode of GNRs overlapping with the incidence excitation wavelength. Surface plasmon effects in the energy transfer were also found in core/shell nanoparticles where gold nanorod cores were coated by dye (Rhodamine 800) doped polystyrene shells [20]. Enhanced energy transfer, indicated by a large decrease in the fluorescence lifetime of fluorophore, was observed when the excitation wavelength matched the longitudinal surface plasmon band of the gold cores. Further energy transfer between Alexa Fluor 405 and gold nanorods under one- and two-photon excitation was demonstrated experimentally using FLIM and theoretically using density matrix method [21]. The energy transfer via the dipole-dipole interaction was found to cause a decrease in the fluorescence lifetime. In this work, a new model for the dipole-plasmon interaction between the dye and metal nanoparticles for the two-photon process was developed where plasmon in the nanorods was considered as localized in all three dimensions (in stead of one-dimensional treatment in surface energy transfer (SET) model) because the size of the nanorod in all

three dimensions is much smaller than the wavelength of the incident light. This description successfully accounts for the surface plasmon enhanced energy transfer under two-photon excitation.

Together these studies demonstrate that gold nanorod-dye energy transfer combinations are appealing, not only in FRET imaging, but also energy transfer-based fluorescence lifetime sensing of bio-analytes. Here, we describe a study of the internalization of GNRs in cells via energy transfer - based fluorescence lifetime imaging using early endosome marker coupled with GFP. Observed energy transfer between GNRs and GFP indicates the involvement of endocytosis in GNR uptake. Moreover, a novel nanoprobe based on functionalized gold nanorod for nucleic acid sensing through energy transfer fluorescence spectroscopy is demonstrated.

II. EXPERIMENTAL

A. Syntheses of Au nanoparticles

Gold nanorods were synthesized by the seeded growth method [22]. To synthesize GNRs, 2.5 ml $HAuCl_4 \cdot 3H_2O$ (0.001 M) and 0.6 ml ice-cold $NaBH_4$ (0.01 M) were added into 7.5 ml cetyltrimethylammonium bromide (CTAB) (0.1 M) to prepare the seeds solution. The growth solution was synthesized by adding 0.15 M BDAC, 25 ml $HAuCl_4 \cdot 3H_2O$ (0.001 M), 1 ml $AgNO_3$ (0.004 M) and 350 µl Ascorbic Acid (0.778 M) to 25 ml CTAB solution (0.1 M). Then 80 µl seed solution (2 hours after preparation) was injected into growth solution to grow gold nanorods. The absorption spectrum shows a longitudinal plasmon mode centered at around 850 nm and a weak transverse plasmon mode at 550 nm.

B. Functionalize Au nanorods with hairpin DNA (hpDNA)

The CTAB surfactant on the GNR surface was first replaced with mercaptohexanoic aic (MHA) using a previously reported round-trip phase transfer ligand exchange approach [23]. Thiolated oligonucleotides and the corresponding complementary oligonucleotides were purchased from Eurofins MWG Operon and Integrated DNA Technologies, respectively. The disulfide bonds of thiolated single strand DNA (ssDNA) were reduced by Tris(2-carboxyethyl)phosphine hydrochloride (TCEP). The MHA-GNRs were conjugated with ssDNA through a salting aging process [24, 25].

C. Cell treatment with gold nanorods

Gold nanorods dispersions were centrifuged to remove the excess CTAB and redispersed in deionized water twice (14000 rpm, 5 mins per cycle) with a final optical density about 1.0. Cells were treated with 100 μl of gold nanorods solution and incubated for 3 hours under standard cell culture conditions at 37 °C and 5% CO_2. The cells were washed thoroughly with phosphate buffered saline (PBS) to remove excess nanorods and fixed with 3.7% paraformaldehyde. After staining with 4'-6-Diamidino-2-phenylindole (DAPI), the sample was dispersed on a glass slide and with a cover slit for imaging.

D. Lifetime Measurements

Time-resolved fluorescence measurements were performed using the time-correlated single-photon counting (TCSPC) technique on an IBH Fluorocube fluorescence lifetime system (Horiba Jobin Yvon IBH Ltd., Glasgow, UK) equipped with emission monochromator. A pulsed light-emitting diode (LED) of 649 nm operating at 1 MHz repetition rate was used as the excitation source. A longpass filter of 670 nm was used to minimize the detection of excitation light. Fluorescence decays were measured at the magic angle (54.7^o) to eliminate polarization effects. Data analysis was performed using nonlinear least squares with the IBH iterative reconvolution software (DAS6 data analysis package). The fluorescence intensity decays were analyzed in terms of the multi-exponential model as the sum of individual single exponential decays:

$$I(t) = \sum_i B_i \exp(-\frac{t}{\tau_i}), \quad [1]$$

where τ_i are the decay times and B_i the associated amplitudes.

The fractional contribution of each lifetime component to the steady-state intensity is represented by

$$f_i = B_i\tau_i / \sum_k B_k\tau_k. \quad [2]$$

E. Fluorescence lifetime imaging microscopy (FLIM)

FLIM was performed by using a confocal microscope (LSM 510, Carl Zeiss) equipped with a time-correlated single photon counting (TCSPC) module (SPC-830, Becker & Hickl GmbH). A femtosecond Ti:Sapphire laser (Chameleon, Coherent) was tuned at 850nm to generate TPL from gold nanorods. The laser pulse has a repetition rate of 80 MHz and duration less than 200 fs. Emission was collected by a 60× water-immersion objective (N.A.=1.0) and a bandpass filter with a transmission window from 500 nm to 550 nm.

III. RESULTS AND DISCUSSION

A. Energy transfer based FLIM study on the internalization of GNRs in HeLa cells

Gold nanoparticles have great potential in biomedical application, including *in vitro* and *in vivo* imaging, sensing, drug delivery and cancer therapy because of their unique physical and chemical properties [26-28]. To exploit the potential, it is essential to understand the penetration of nanoparticles through biological barriers [29]. The study of intracellular pathways of gold nanoparticles and uptake mechanisms are critical for many of these applications, as they provide information on uptake rate, route, final intracellular location, the effects of nanoparticles to cell organelles, etc. However this is not a trivial task. On one hand, the uptake process is a complex process influenced by both the properties of cells, such as cell groups and types, and characteristics of nanoparticles, such as the size, shape, surface charge and coating conditions [30-39]. So far different nanoparticle pathways into cell membranes have been reported and mechanisms are still a subject of study [40, 41]. On the other hand, conventional techniques used for tracking nanoparticles in cell cultures have both advantages and limitations. For example, traditional fluorescence microscopy can perform *in vivo* or *in vitro* imaging on cell organelles via fluorescence labeling, but it is restricted by its diffraction-limited spatial resolution. It is difficult in some cases to conclude whether the overlapping pixel is real colocalization or just structures in approximation. Super resolution techniques can extend the limit of optical microscopy but only at a considerable increase in complexity. Similarly, transmission electron microscopy (TEM) has superior spatial resolution but the specimen has to be thinly sliced and imaged under vacuum, therefore is not suitable for *in situ* visualization of biological samples.

Here we introduce a two-photon energy transfer - based FLIM method that monitors the energy transfer between gold nanorods and fluorescent molecules in order to study cell uptake of GNRs. As the energy transfer process only occurs when two fluorophores are in close approximation (typically within 8 nm for Förster resonance energy transfer and double this distance for surface energy transfer), this FLIM-FRET method can directly indicate whether gold nanoparticles are enclosed in a specific cellular organelle, e.g., endosomes, and can be applied both *in vivo* and *in vitro*. TPL and energy transfer process have been combined to study the involvement of endocytosis in intra-cellular trafficking of gold nanorods in HeLa cells. Invitrogen CellLight® Early Endosomes-GFP, BacMam 2.0 kit, was used in this work. BacMam 2.0 kit offers a user-friendly technique which contains protein fusion of green fluorescent protein (GFP) and early endosome marker RAB5a. HeLa cells were treated with 5% GNRs (volume ratio) and the BacMam kit for 1 hr then fixed for imaging experiments.

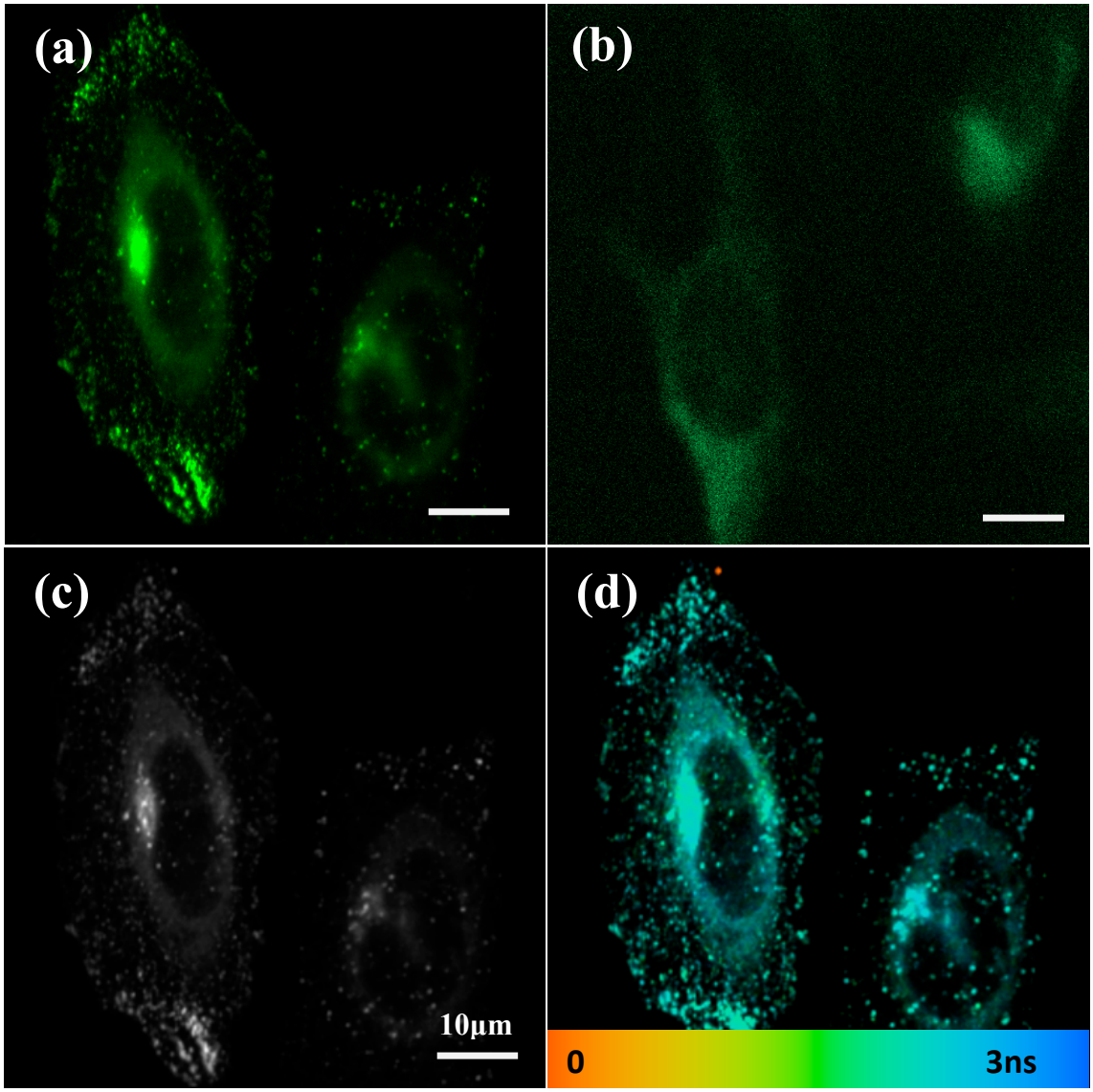

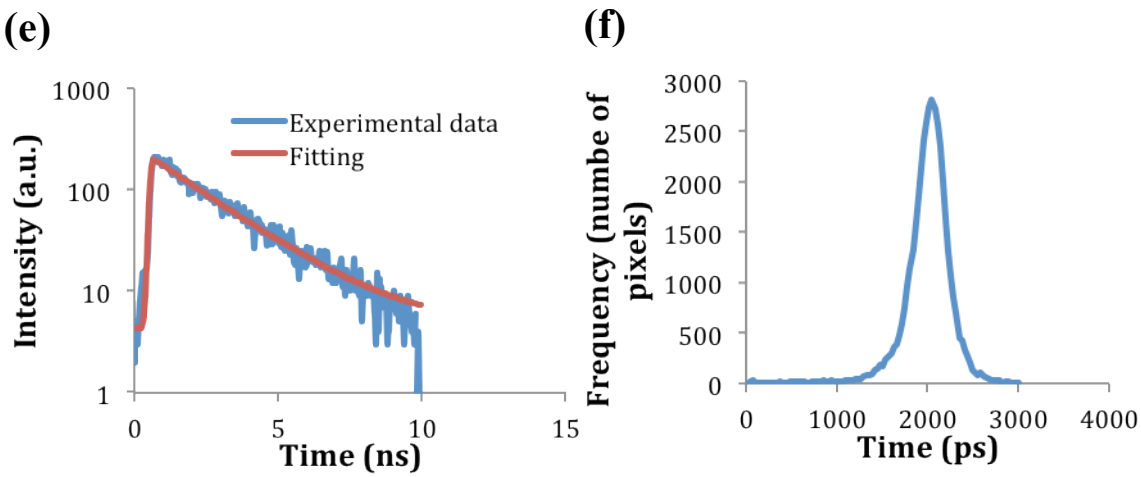

Fig.1 (a) Confocal fluorescence image of HeLa cells treated with Rab5a-GFP, excited at 488 nm, emission collected with a longpass 505 nm filter; (b) HeLa cells without Rab5a-GFP; (c), (d) Intensity

and FLIM image of two-photon excited HeLa cells treated with Rab5a-GFP, excited under 850 nm and emission collected with 500-550 nm bandpass filter. For FLIM image, the lifetime ranges from 0 (orange) to 3ns (blue); (e) Typical decay curve of fluorescence from GFP in cell culture; (f) Distribution of fluorescence lifetimes displayed in (d). The same scale bars for (a), (b), (c) and (d). The luminescence intensity in (a) and (b) are indicated by the brightness of the images from 0 (dark) to 255 (bright green spots in (a)).

Fig. 1 (a) shows a typical confocal image of HeLa cells labelled by Rab5a-GFP. Bright spots in the image are considered to be fluorescence from GFP, while no strong fluorescence signal but only weak cell autofluorescence can be seen from a control sample in Fig. 1(b). Fig.1 (c) is a TPL intensity image taken from the same sample as in Fig. 1 (a) with 850 nm femto-second laser excitation and 500-550 nm emission bandpass filter. Fig. 1 (d) is the FLIM image of the same area where different colours in each image pixel varying from orange to blue represent fluorescence lifetimes ranging from 0 to 3 ns. The fluorescence lifetime was obtained by fitting the experimental decay curves to a single exponential decay model, as shown in Fig. 1 (e). The fluorescence lifetime of GFP in cell culture is found to be around 2 ns with a symmetric distributionin (Fig. 1 (f)), consistent with previous reports [43, 44]. Fig. 1 shows that Rab5a-GFP allowed imaging of early endosomes in HeLa cells and emitted strong and stable fluorescence under both single and two-photon excitations.

To investigate the uptake process of gold nanorods by HeLa cells, we have incubated the cells with gold nanorods at 5% volume concentration under 37 °C for different time periods, from 30 minutes to 1 hour. FLIM images are shown in Fig. 2: from (a) to (c), the gold nanorods incubation time is 30 minutes, 45 minutes, and 1 hour respectively. Decay curves of all bright pixels in images have been fitted by a two-exponential model as the luminescence from gold nanorods has to be considered. The coded colour hereby represents the average lifetime τ_{ave}, which can be expressed by $\tau_{ave} = \sum_i^n B_i \tau_i$ (n=2). In the FLIM images, green/blue pixels are emission from GFP, while brighter orange/yellow spots in cells are considered to be signals from gold nanorods or overlapping areas where both emissions from GNRs and GFP were found. This is because that the decay time scale of TPL from GNRs [18] is extremely small (<100 ps and comparable to the instrumental impulse response), while the intensity is much stronger than that from GFP (contribution over 80% of total signal). Therefore even though the lifetime of GFP is as long as 2 ns, the average lifetimes in these pixels are quite short, usually around several hundred picoseconds.

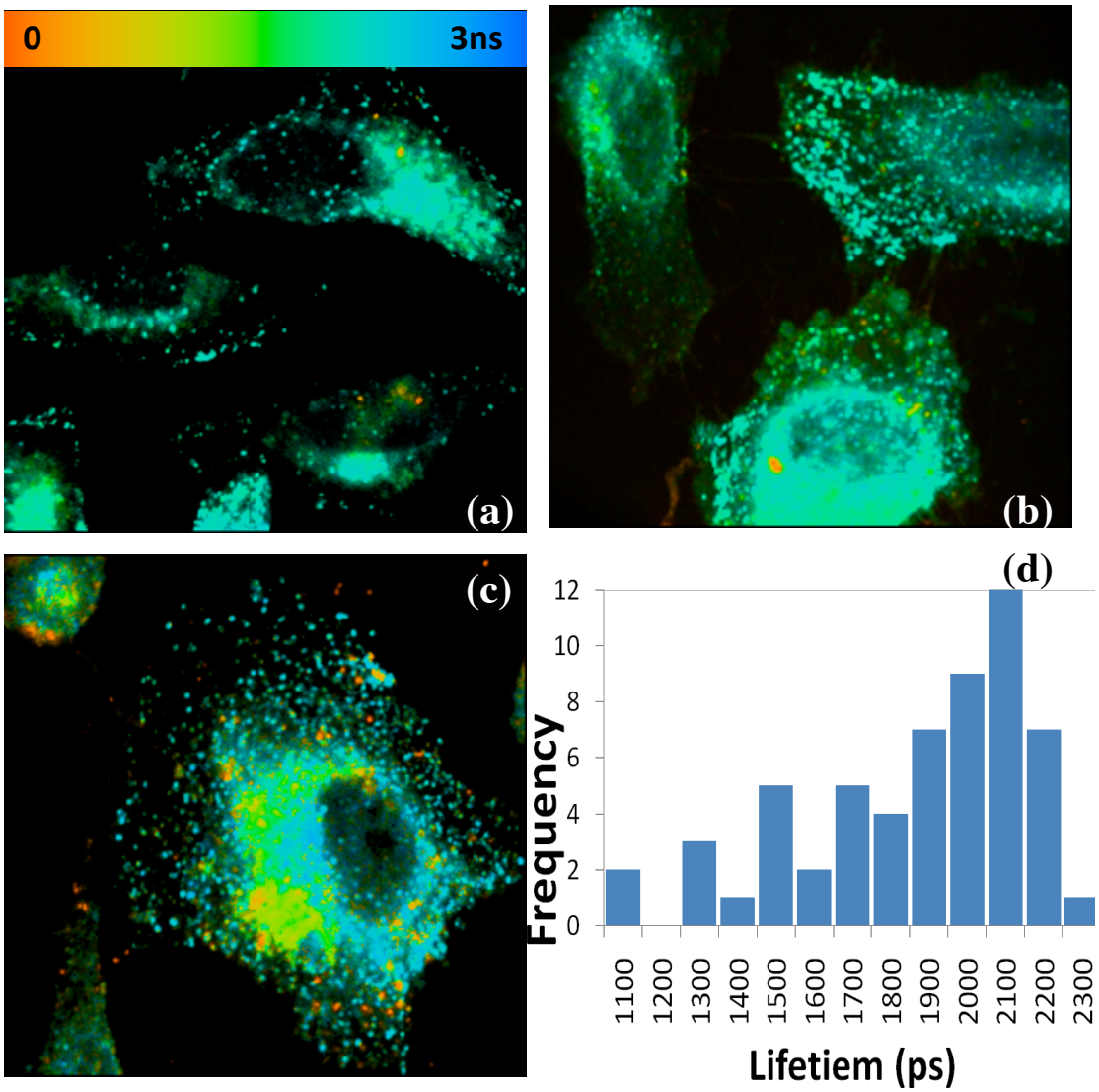

Fig.2 FLIM images of Rab5a-GFP treated HeLa cells incubated with CTAB capped gold nanorods for (a) 30 minutes, (b) 45 minutes, and (c) 1 hour; (d) Lifetime distribution of GFP in overlapping areas.

Fig. 2 shows that a few gold nanorods were found in cells after incubation for 30 min and 45 min, while significant amount of nanorods have been found in cells after 1 hr incubation, demonstrated by the increasing in number of the pixels displaying shorter lifetime, i.e., orange color. All the bright spots in FLIM images are found to be overlapping pixels, i.e., GNRs overlap with Rab5a-GFP stained early endosomes and there are no isolated GNRs. A further analysis of the FLIM image has been carried out to examine whether there was energy transfer between GFPs and GNRs in order to confirm the involvement of early endosome in the uptake process. To this end, the long lifetime component originating from GFP in the overlapping areas was analysed. As shown in Fig. 2 (d), the long lifetime component subtracted from 58 overlapping pixels in different FLIM images have been sorted in 100 ps

interval from 1100 ps to 2400 ps. Compared to a symmetric lifetime distribution of GFP (Fig. 1 (f)), lifetimes of GFP in the vicinity of gold nanorods form an asymmetric distribution, showing a higher rate of reduced lifetime with a long tail reaching 1.1 ns, which suggests energy transfer does exist between GFP and gold nanorods. This indicates that gold nanorods and Rab5a-GFP are in close proximity, implying the cell uptake of gold nanorods by endocytosis.

B. Gold nanorod - based energy transfer probe for RNA sensing

Messenger ribonucleic acid (mRNA) bridges genome information harboured within DNA to phenotypes primarily and collectively expressed by proteins. In most cases, the dynamics of mRNA in the cell directly reflects the levels of protein, hence the phonotypical expression. Because of its important roles in biology numerous methods have been developed to assess the mRNA expression in response to a variety of physiological and pathological cues [42-44]. Molecular beacon (MB) is one of the most promising probes for mRNA detection. MB is usually designed with a hairpin-structured oligonucleotide with a fluorophore-quencher pair that undergoes a spontaneous fluorogenic conformational change upon hybridization with the complementary nucleic acid target [45, 46]. MB offers good opportunities in homogeneous assays of mRNA and real-time monitoring of the expression of mRNA inside living cells due to its good sensitivity and enhanced specificity [47-50]. However, traditional MBs suffer from problems of lacking universal organic quenchers [51]. Quenching efficiency may vary from one fluorophore to another, limiting the signal/background ratio. Moreover, transfection reagents are required for cellular internalization of MBs. Recent studies show that these limitations can be elegantly addressed by using functionalized gold nanoparticles (AuNPs). It has been proven that AuNPs are highly efficient quenchers for a range of organic fluorophores [48] and exhibit long-range fluorescence quenching capability [15,21,52]. Moreover, AuNPs functionalized by oligonucleotides show highly efficient cellular uptake without the need of transfection reagents and extraordinary intracellular stability against enzymatic degradation as well as enhanced binding capability of complementary nucleic acids [53-55]. Exploring the potential of gold nanoparticle based RNA probes, here we report a new nanoprobe based on functionalized gold nanorods and the influence of hairpin structure on the quenching efficiency of this energy transfer pair.

Thiolated oligonucleotides and the corresponding complementary oligonucleotides used in this work are listed in Table 1. The underlined bases represent the stem sequences in their hairpin structure. Fig. 3 shows fluorescence decay curves taken from hairpin DNA (hpDNA) functionalized GNRs in their initial quenching states. Lifetime analysis using multiple exponentials reveals three lifetime components, as

summarized in Table 2. Two lifetime components were found in the ns and sub ns range that can be attributed to Cy5, while the third short lifetime component in the tens of ps region is probably due to strong scattering from gold cores. Three probes, namely hpCy5_2, hpAACy5 and hpCy5f, have first lifetime components, 1.6 ns, 0.9 ns and 1.2 ns, shorter than the lifetime found from these Cy5 – oligonucleotide in free form (2.1 ns, 1.8 ns and 2.0 ns, respectively). In contrast, the first lifetime component of hpCy5_1 (1.8 ns) is comparable to its free form (1.96 ns). This suggests the existence of loosed hairpins possibly due to a relatively low hairpin melting temperature (48.2 ^{o}C). The second lifetime component of all four samples are in sub nanosecond range, indicating much reduced lifetimes arising from energy transfer between Cy5 and GNRs. Detailed comparison reveals that hpAACy5 surpasses other designs and has the highest energy transfer efficiency. This is resulted from a short distance between Cy5 and gold surface because hpAACy5 has only 2As while the other three designs have 5 or more Ts at the 3$^{'}$ end. This improvement in the quenching efficiency results in a reduced background and thus an enhanced signal/background ratio. Fig. 4 compares the fluorescence spectra taken from GNR-hpCy5_2 and GNR-hpAACy5 before and after hybridization with their complementary oligonucleotides. An apparent increase in fluorescence intensity is observed in both cases, suggesting a successful switching from initial quenching states to final fluorescence states after hybridization. As expected, hpAACy5 probe has a higher signal/background ratio than hpCy5_2 does. For the first time, this study shows that time-resolved fluorescence spectroscopy is a useful tool for investigating the quenching efficiency of hairpin DNA functionalized gold nanorods and reveals the significance of hairpin design on the performance of such a nanoprobe. It is anticipated that this study will bring insight to the optimization of such RNA nanoprobes.

IV. Conclusion

In summary, we have found that energy transfer provides more additional information in biological studies when combined with the advantages of two-photon excitation microscopy of GNRs, as demonstrated here in the study of intra-cellular trafficking of GNRs in HeLa cells via GFP labelled early endosome. GNRs would seem to have further potential, not only in FRET imaging, but also in fluorescence lifetime-based intra-cellular sensing of bio-analytes. A new RNA probe based on hairpin DNA functionalized GNR has been demonstrated. This method combines the strength of enhanced energy transfer in GNRs-dye pairs and TPL of GNRs, in addition to other advantages of GNRs, such as photostability, self-uptaken by cells, multiplexing and multifunctional capability, overcoming the technical limits suffered by other fluorogenic methods, e.g., fluorescence protein labelling and hybrid fluorescence probes. This new mRNA probe thus potentially opens up new possibilities in cancer

diagnosis and prognosis. We have also demonstrated that time-resolved fluorescence spectroscopy can be applied to investigate the influence of hairpin design on the initial quenching state and thus bring insight towards optimizing such nanoprobes.

Table 1. DNA Sequences Used in This Work.

Name	Sequence (5' to 3')[a]	Hairpin T_m (^{o}C)[b]	Hairpin ΔG (kcal/mol)[b]
hpCy5_1	Cy5-CCGAG TTG GTG AAG CTA ACG TTG AGG CTCGG TTTTT-SH	48.2	-3.28
hpCy5_2	Cy5-CCGGTG GTG AAG CTA ACG TTG AG CACCGG TTTTT-SH	60.5	-5.66
hpAACy5	Cy5-CTGACTTG GTG AAG CTA ACG TTG AG CAAGTCAG AA-SH	58.9	-6.58
hpCy5f	Cy5-AATTT AAATTGAACTTG GTG AAG CTA ACG TTG AG CAAGTTCAATTT TTT TTT TTT T-SH	60.5	-10.12
cDNA_1[c]	CCT CAA CGT TAG CTT CAC CAA		
cDNA_2[d]	CTC AAC GTT AGC TTC AC		

[a] The underlined bases represent the stem sequence.
[b] Predicted at 25 ^{o}C in 100 mM [Na^+] buffer by UNAFold software (www. idtdna.com).
[c] Complementary DNA for hpCy5_1.
[d] Complementary DNA for hpCy5_2, hpAACy5 and hpCy5f.

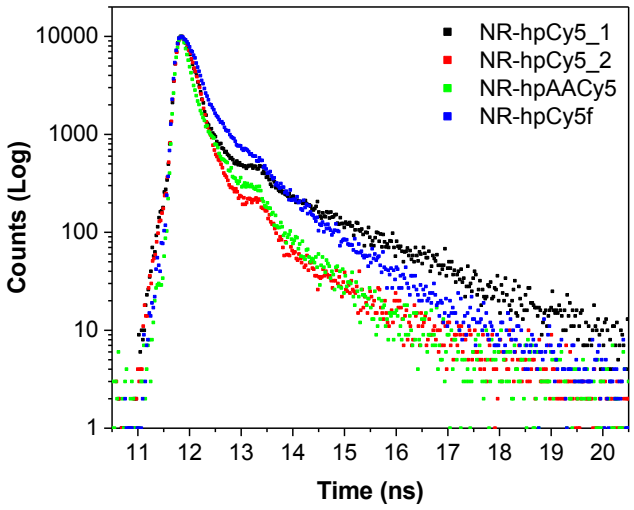

Fig. 3 Fluorescence decay curves taken from hpDNA functionalized GNRs in their initial quenching states.

Table 2. Fluorescence lifetimes from a three exponential model fitting

SAMPLE	τ_1 (NS)	B_1 REL. AMPL	τ_2 (NS)	B_2 REL. AMPL	τ_3 (NS)	B_3 REL. AMPL	X^2
GNR-HPDNA-CY5_1	1.803 ± 0.020	17.91 %	0.326 ± 0.022	8.49 %	0.034 ± 0.004	73.60 %	1.14
GNR-HPDNA-CY5_2	1.629 ± 0.052	5.22 %	0.290 ± 0.011	15.38 %	0.055 ± 0.002	79.39 %	1.03
GNR-HPAACY5	0.942 ± 0.022	13.39 %	0.238 ± 0.008	31.25 %	0.030 ± 0.005	55.36 %	1.56
GNR-HPDNA-CY5F	1.225 ± 0.021	17.27 %	0.408 ± 0.021	24.98 %	0.057 ± 0.002	57.75 %	1.26

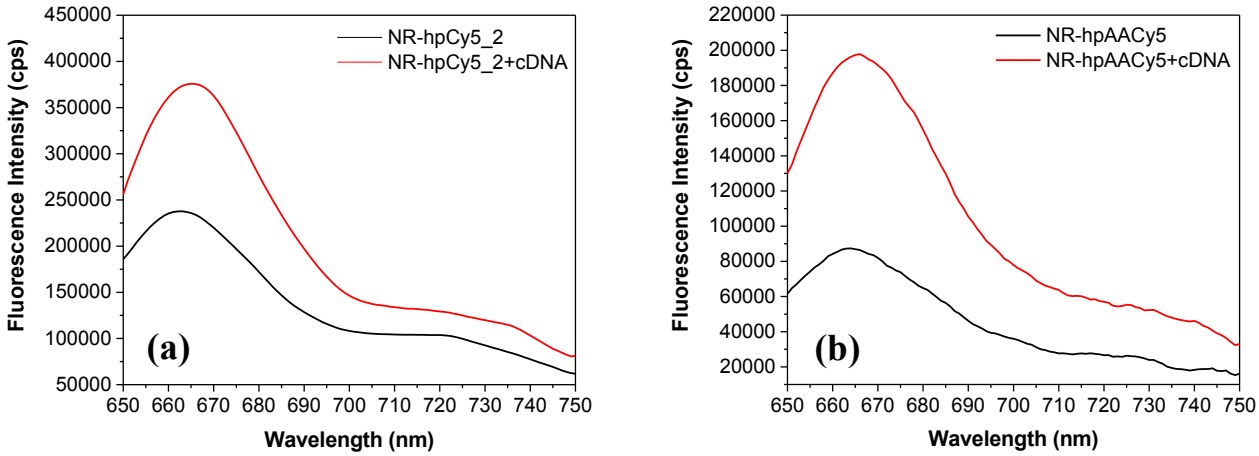

Fig. 4 Fluorescence spectra taken from (a) GNR-hpCy5_2 and (b) GNR-hpAACy5 before (black) and after (red) hybridization with their complementary oligonucleotides (500 nM).

V. Acknowledgement

The authors acknowledge W. Li and R. Y. M. M. Qotob for assistance during the experimental work. This work was supported by a BBSRC Award BB/K013416/1. G. Wei acknowledges financial support from China Scholarship Council (CSC).

References

[1] O. J. Rolinski, D. J. S. Birch, L. J. McCartney, J. C. Puckup, *J. Photochem. And Photobiol. B* 2000, **54**, 26-34.
[2] A. J. W. G. Visser, S. P. Laptenok, N. V. Visser, A. van Hoek, D. J. S. Birch, J-C Brochon, J. W. Borst, *Eur. Biophys. J.* 2010, **39**, 241-53.
[3] C. S. Yun, A. Javier, T. Jennings, M. Fisher, S. Hira, S. Peterson, B. Hopkins, N. O. Reich, G. F. Strouse, *J. Am. Chem. Soc.* 2005, **127**, 3115.
[4] X. Huang, S. Neretina, M. A. El-Sayed, *Adv. Mater*. 2009, **21**, 4880-4910.
[5] P. K. Jain, X. Huang, I. H. El-Sayed, M. A. El-Sayed, *Accounts Chem. Res.* 2008, **41**, 1578-158.
[6] Y. Chen, Y. Zhang, D. J. S. Birch, A. S. Barnard, *Nanoscale* 2012, **4**, 5017.
[7] Y. Zhang, D. Xu, W. Li, J. Yu, Y. Chen, *J. Nanomater*. 2012, 375496.
[8] Y. Zhang, J. Yu, D. J. S. Birch, Y. Chen, *Proc. SPIE* 2011, 7910 79101H.
[9] S. Link, M. A. El-Sayed, *Int. Rev. in Phys. Chem*. 2000, **19** (3), 409- 453.
[10] M. B. Mohamed, V. Volkov, S. Link, M. A. El-Sayed, *Chem. Phys. Lett.* 2000, **317,** 517–523.
[11] R. A. Farrer, F. L. Butterfield, V. W. Chen, J. T. Fourkas, *Nano Lett.,* 2005, **5,** 1139-1142.
[12] H. Wang, T. B. Huff, D. A. Zweifel, W. He, P. S. Low, A. Wei, J. Cheng, *Proc. Nat. Acad. Sci. USA* 2005, **102**, 15752–15756.
[13] K. Imura, T. Nagahara, H.mi Okamoto, *J. Phys. Chem. B* 2005, **109**,13214-13220.
[14] X. H. Huang, I. H. El-Sayed, W. Qian, M. A. El-Sayed, *J Am. Chem. Soc.* 2006, **128,** 2115-2120.
[15] Y. Zhang, D. J. S. Birch and Y. Chen, *Appl. Phys. Lett*. 2011, **99**, 103701.
[16] X. H. Huang, S. Neretina, M. A. EL-Sayed, *Adv. Mater*. 2009, **21**, 4880.
[17] Y. Chen, J. A. Preece and R. E. Palmer, *Ann. N. Y. Acad. Sci.* 2008, **1130**, 201.
[18] Y. Zhang, J. Yu, D. J. S. Birch, Y. Chen, *J. Biomed. Opt*. 2010, **15**, 020504-3.

[19] T. Sen and A. Patra, *J. Phys. Chem. C* 2012, **116**, 17307−17317.
[20] P. Gu, D. J. S. Birch and Y. Chen, Methods Appl. Fluoresc. 2014, **2**, 024004.
[21] C. Rachnor, M. R. Singh, Y. Zhang, D. J. S. Birch and Y. Chen, Methods Appl. Fluoresc. 2014, **2**, 015002.
[22] J. Murphy, T. K. Sau, A. M. Gole, C. J. Orendorff, J. Gao, L. Gou, S. E. Hunyadi, T. Li, *J. Phys. Chem. B*. 2005, **109**, 13875.
[23] A. Wijaya and K. Hamad-Schifferli, *Langmuir*, 2008, **24**, 9966–9.
[24] S. J. Hurst, A. K. R. Lytton-Jean, and C. A. Mirkin, Anal. Chem., 2006, **78**, 8313–8.
[25] A. Wijaya, S. B. Schaffer, I. G. Pallares, and K. Hamad-Schifferli, ACS Nano, 2009, **3**, 80–6.
[26] V. Biju, *Chem. Soc. Rev*., 2014, **43**, 744.
[27] T. Bose, D. Latawiec, P. P. Mondal and S. Mandal, *J. Nanopart Res.* 2014, **16**, 2527.
[28] L. A. Austin, M. A. Mackey, E. C. dreaden, M. A. Ei-Sayed, *Arch Toxicol*, 2014, **88**,1391-1417.
[29] S. Barua and S. Mitragotri, *Nano Today,* 2014, **9**, 223-243.
[30] A. E. Nel, L. Mädler, F. Velegol, T. Xia, E. M. V. Hoek, P. Somasundaran, F. Klaessig, V. Castranova, M. Thompson, *Nat. Mater.* 2009, **8**, 543-557.
[31] S. J. H. Soenen, M. D eCuyper, *Nanomedicine,* 2010, **5**, 1261.
[32] S. D. Conner, S. L. Schmid, *Nature*, 2003, **422**, 37-44.
[33] J. Davda, V. Labhasetwar, *Int. J. Pharm.* 2002, **233**, 51-59.
[34] T. Kato , T. Yashiro , Y. Murata , D. C. Herbert , K. Oshikawa, M. Bando, S. Ohn , Y. Sugiyama, *Cell Tissue Res.* 2003, **311**, 47-51.
[35] A. T. Florence, N. Hussain, *Adv. Drug Deliv. Rev.* 2001, **50**, S69-S89.
[36] F. Zhao, Y. Zhao, Y, Liu, X. Chang, C. Chen, Y. Zhao, *Small*, 2011, **7**, 1322-1337.
[37] A. Verma, F. Stellacci, *Small,* 2010, **6**, 12-21.
[38] H. J. Parab, H. M. Chen, T. C. Lai, et al., *J. Phys. Chem. C.,* 2009, **113**, 7574-7578.
[39] J. H. Huang, T. C. Lai, L. C. Cheng, et al., *J. Mater. Chem*., 2011, **21**, 14821-14829
[40] Z. Liu, W. Cai, L. He, N. Nakayama, K. Chen, X. Sun, X. Chen, H. Dai, *Nat. Nanotechnol.* 2007, **2**, 47-52.
[41] V. Mailänder, K. Landfester, *Biomacromolecules*, 2009, **10**, 2379-2400.
[42] D. Sivaraman, P. Biswas, L. N. Cella, M. V. Yates and W. Chen, *Trends in Biotech.* 2011, **29**, 307.
[43] B. A. Armitage, *Current Opinion in Chem. Bio*. 2011, **15,** 806.
[44] S. R. Harry, D. J. Hicks, K. I. Amiri and D. W. Wright, *Chem. Commun*., 2010, **46,** 5557.
[45] S. Tyagi, F. R. Kramer, *Nat. Biotechnol.* 1996, **14**, 303–308.
[46] S. Tyagi, D. P. Bratu and F. R. Kramer, *Nat. Biotechnol.* 1998, **16**, 49–53.
[47] T. Matsuo, *Biochim. Biophys. Acta* 1998, **1379**, 178–184.
[48] D. L. Sokol, X. Zhang, P. Lu, A. M. Gewirtz, *Proc. Natl. Acad. Sci.* 1998, ***95***, 11538–11543.
[49] N. Nitin, P. J. Santangelo, G. Kim, S. Nie, G. Bao, *Nucleic Acids Res.* 2004, **32**, e58.
[50] C. D. Medley, T. J. Drake, J. M. Tomasini, R. J. Rogers, W. Tan, *Anal. Chem.* 2005, **77**, 4713–4718.
[51] B. Dubertret, M. Calame, A. J. Libchaber, *Nat. Biotechnol.* 2001, **19**, 365–370.
[52] S. Mayilo, M. A. Kloster, M. Wunderlich, A. Lutich, T. A. Klar, A. Nichtl, K. Kürzinger, F. D. Stefani, J. Feldmann, *Nano Lett.* 2009, **9**, 4558–4563.
[53] N. L. Rosi, D. A. Giljohann, C. S. Thaxton, A. K. E. Lytton-Jean, M. S. Han, C. A. Mirkin, *Science* 2006, **312,** 1027–1030.
[54] D. S. Seferos, D. A. Giljohann, H. D. Hill, A. E. Prigodich, C. A. Mirkin, *J. Am. Chem. Soc.* 2007, **129,** 15477–15479.
[55] A. E. Prigodich, D. S. Seferos, M. D. Massich, D. A. Giljohann, B. C. Lane, C. A. Mirkin, *ACS Nano* 2009, **3**, 2147–2152.
[¶] current address, College of Physics, Jilin University, 2699 Qianjin Street, Changchun 130012, China